RSC Advances

PAPER

View Article Online
View Journal | View Issue

Cite this: *RSC Adv.*, 2017, **7**, 5222

Reinforcing biofiller "Lignin" for high performance green natural rubber nanocomposites†

Yuko Ikeda,*[a] Treethip Phakkeeree,[b] Preeyanuch Junkong,[b] Hiroyuki Yokohama,[b] Pranee Phinyocheep,[c] Ritsuko Kitano[d] and Atsushi Kato[d]

Received 5th November 2016
Accepted 31st December 2016

DOI: 10.1039/c6ra26359c

www.rsc.org/advances

High performance eco-friendly natural rubber biocomposites filled with 5, 10, 20, and 40 parts per one hundred rubber by weight (phr) of lignin were prepared from sodium lignosulfonate and natural rubber (NR) latex using the soft processing method. The formation of network-like lignin structures was detected around the rubber phases even when the amount of lignin was increased to 40 phr. The Payne effect clearly suggested the presence of filler–filler interaction of lignin in the biocomposites. The distinguishably superior reinforcement effects of lignin at different levels of content were clearly apparent in the biocomposites. Specifically, the tensile stresses of the biocomposites significantly increased with an increase in the lignin content. Under dynamic conditions, the biocomposites showed larger storage moduli and lower dissipative loss with low glass transition temperatures with increasing amount of lignin. The generation of crystallites by strain-induced crystallization (SIC) was evaluated by using quick time-resolved wide-angle X-ray diffraction/tensile measurements, and a stepwise SIC phenomenon was observed for the lignin-filled NR soft biocomposites. This is a first report on the organic filler filled NR nanocomposite. The lignin content did not significantly affect the generation of crystallites of the NR biocomposites. This characteristic could strongly influence the development of rubber science and technology. Sodium lignosulfonate will be applicable as a good reinforcing biofiller for the preparation of green NR nanocomposites.

Introduction

There is rising consciousness about the environment, depletion of petroleum resources, and related health concerns. Therefore, the development of sustainable materials derived from biorenewable resources has come into focus. Natural rubber (NR) is an essential sustainable soft material. It is the only agricultural product among rubbers, and the only polymeric hydrocarbon derived from the biological world.[1] NR can be continuously produced even after the depletion of fossil fuels (petroleum and coal). NR is known to exhibit various outstanding properties on the basis of its high elasticity due to entropy.[2–4] The characteristics of NR cannot be easily mimicked by synthetic rubbers, even though polymer science and technology have significantly developed in the last century.

NR-based soft composites have been regarded as one of the most successful materials for industrial products among many polymer composites. In terms of sustainable development and carbon-neutral products, biofillers such as cellulose nanofibres, biosilica, and lignin have attracted the attention of many researchers. Among them, lignin is the second most abundant biopolymer after cellulose. The effective use of lignin waste from kraft processes is gaining focus.[5,6] Typically, lignin from kraft process is used as a low value fuel in paper-pulp manufacturing.[7–9]

Lignin is a three-dimensional amorphous natural polymer, which is generally contained in woods at approximately 15–25% by weight. It provides the strength in the wood to protect against mechanical and biological stresses. The major chemical functional groups in lignin are dependent on its genetic origin, and applied extraction processes.[10] The chemical constituents and network structure of lignin are different depending on its extraction process. These characteristics have been shown to confer special functional properties on lignin, such as a stabilizing effect,[11] reinforcing effect, biodegradability, anti-fungal property, antibiotic activity,[11–14] and UV-absorption.[15]

Extensive trials have also been carried out for using lignin waste as a filler component in rubbery composites, which is a promising reuse of lignin waste.[5,6] However, lignin from waste was found unsatisfactory for the reinforcement of rubber materials due to the difficulty of blending lignin with other systems.[15–18] Thus, most of the lignin waste needed to be modified, for example, into fabricated lignin by using graft copolymerization, lignin-cationic polyelectrolyte complexes, *etc.*, in order to improve compatibility with

[a]*Faculty of Molecular Chemistry and Engineering, Kyoto Institute of Technology, Matsugasaki, Sakyo, Kyoto 606-8585, Japan. E-mail: yuko@kit.ac.jp*
[b]*Graduate School of Science and Technology, Kyoto Institute of Technology, Matsugasaki, Sakyo, Kyoto 606-8585, Japan*
[c]*Department of Chemistry, Faculty of Science, Mahidol University, Rama VI Road, Ratchthewee, Bangkok 10400, Thailand*
[d]*NISSAN ARC, LTD., Natsushima-cho 1, Yokosuka, Kanagawa 237-0061, Japan*

† Electronic supplementary information (ESI) available: The videos of three-dimensional LSCM images for NR-L40-S-soft and NR-L40-S-mill samples. See DOI: 10.1039/c6ra26359c

rubber and other polymer matrices.[5,6,18] Up to now, there is inadequate information on lignin-reinforced polymer composites.[5,6] Therefore, development of eco-friendly and sustainable materials requires a more effective use of lignin.

Is it truly difficult for lignin to be used for rubber reinforcement? To answer this question, a trial was conducted to use a soft processing method, and preliminary results were reported in our rapid communication.[19] Our group that conducted this research focused on the soft processing method, which takes advantage of NR latex, to prepare novel high-performance NR composites.[20] The method is based on the idea that a filler network is formed in an NR matrix by using NR particles in the NR latex as a template. The reinforcement effect of the filler network for NR has been recognized as being useful; for example, the role of the filler network in the high performance of *in situ* silica/NR nanocomposites was clearly shown using this technique.[21,22] Lignin was also successfully used as an effective reinforcing filler for NR, similar to inorganic fillers, in which 10 parts per one hundred rubber by weight (phr) of lignin was mixed with NR latex using this soft processing method.[19] This method is very simple and can be easily utilized for practical rubber production applications. The characteristics of only 10 phr lignin-filled NR nanocomposite were also briefly reported in the rapid communication.[19] The present study investigates the effect of lignin content on the tensile properties of lignin-filled NR composites, with their unique morphological features. The results will be useful in revealing the role of organic filler "lignin" for the reinforcement of NR.

Experimental section

Materials

Commercial NR latex with 0.7% of NH_4OH, and a dry rubber content (DRC) of 60% was purchased from Thai Rubber Latex Public Co., Ltd., Thailand. Sodium lignosulfonate (Pearllex NP with the content of sulfonate group; 1.8 mmol g^{-1}) from Nippon Paper Chemicals, Co., Ltd., Japan was used as received. Analytical grade sodium hydroxide was purchased from Labscan Co., Ltd., Thailand. Vulcanizing reagents were zinc oxide (ZnO), zinc diethyl dithiocarbamate (ZDEC), and sulfur (S_8) from Luckyfour Co., Ltd., Thailand.

For conventional mixing, solid NR (RSS no. 1) was used. Elemental sulfur (powder, 150 mesh), stearic acid (LUNAC S-25), ZnO (average diameter 0.29 μm), and *N*-(1,3-benzothiazol-2-ylsulfanyl)cyclohexanamine (CBS) (Sanceler CM-G) were commercial grades for rubber industry and used as received. They were supplied from Hosoi Chemical Industry Co., Ltd., Kao Co., Sakai Chemical Industry Co., Ltd., and Sanshin Chemical Industry Co., Ltd., respectively.

Preparation of Lignin/NR biocomposites by soft processing method

Novel biocomposites composed of lignin and NR were prepared by the soft processing method: high ammonia NR latex of 100 ml was mixed with 50% sulfur dispersion of 1.5 phr, 50% ZDEC dispersion of 1.0 phr and 50% ZnO dispersion of 1.8 phr at r.t. in advance, and followed by mixing with each alkali aqueous solution of 5, 10, 20 or 40 phr of sodium lignosulfonate, respectively. Because the sodium lignosulfonate from kraft process was hydrophobic,[23] it was soluble in some organic solvents and was practically insoluble in water. Thus, it was difficult to mix the lignin powder with the NR latex directly. However, the sodium lignosulfonate was soluble in an aqueous NaOH solution. In addition, the NR latex was preserved by NH_4OH, and the basic condition of NR latex was preferable for the mixing. Therefore, the sodium lignosulfonate solution was prepared by stirring in an aqueous NaOH solution of 0.1 mol l^{-1} at first. The final concentration of lignin solution was 30 w/v%. The biocomposite films were prepared by casting the liquid mixture on a glass plate, and they were evaporated at r.t. for a few days. The obtained films were subjected to cross-linking at 70 °C for 4 h, and were dried at r.t. under a reduced pressure. The biocomposites having lignin of 5, 10, 20 and 40 phr are abbreviated as NR-L5-S-soft, NR-L10-S-soft, NR-L20-S-soft and NR-L40-S-soft, respectively. In addition, an unfilled sample (NR-L0-S-soft) was also prepared by the soft processing method as a reference. In the sample codes, "L", "number", "S" and "soft" mean lignin, a content of lignin in phr, a sulfur cross-linking, and the soft processing, respectively.

As reference samples, lignin-filled NR biocomposites were prepared from solid NR and lignin powder by the conventional method. ZnO of 1.8 phr, stearic acid of 2.0 phr, CBS of 1.0 phr, sulfur of 1.5 phr and lignin 5, 10, 20, or 40 phr were mixed with solid NR on a two-roll mill at r.t. for sulfur cross-linking. Each rubber compound was molded into a sheet of 1 mm thickness by heat pressing at 140 °C for 12 min, which was the optimal cure time determined by the cure measurement at 140 °C by JSR Curelastometer III. The biocomposites having lignin of 5, 10, 20 and 40 phr are abbreviated as NR-L5-S-mill, NR-L10-S-mill, NR-L20-S-mill and NR-L40-S-mill, respectively. An unfilled NR sample (NR-L0-S-mill) was also prepared by using the same recipe. In the sample codes, "L", "number", "S" and "mill" mean lignin, a content of lignin in phr, a sulfur cross-linking, and conventional mixing method, respectively.

Measurement of network-chain density

A network-chain density (ν) of the films of lignin-filled NR biocomposites was evaluated on the basis of the classical theory of rubber elasticity as follows;[24]

$$\sigma = \nu RT\left(\alpha - \frac{1}{\alpha^2}\right) \quad (1)$$

where σ is tensile stress, R is gas constant, α is stretching ratio and T is absolute temperature.

Raman spectroscopy

NR-L10-S-soft and NR-L40-S-soft were directly subjected to Raman spectroscopy without any treatments by Nicolet iS50 FT-IR with the Raman module (Thermo Fisher Scientific Inc.) using diode laser at 1064 nm. The resolution and accumulation time were 8 cm^{-1} and 500 times, respectively. Raman spectral bands of NR-L0-S-soft, NR-L10-S-soft and NR-L40-S-soft are shown in

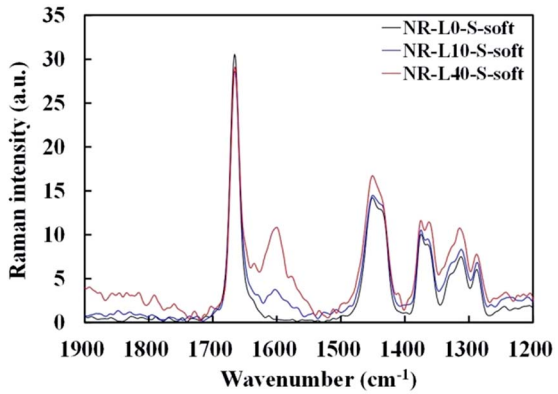

Fig. 1 Raman spectra of NR-L0-S-soft, NR-L10-S-soft and NR-L40-S-soft.

Fig. 1. The bands indicating hydrocarbon chains of *cis*-1,4-polyisoprene of NR, were assigned at $\nu = 1666$ cm^{-1} (C=C stretching), 1288 cm^{-1} (CH bending), 1375 cm^{-1} (CH_3 asymmetric deformation), 1451 and 1362 cm^{-1} (CH_2 deformation), and 1315 cm^{-1} (CH_2 twisting). In addition, the Raman spectral bands which are contributed to lignin were found at $\nu = 1600$ cm^{-1} (C–C of aromatic ring symmetric stretching), 1635 cm^{-1} (probably ascribable to C=C stretching of coniferaldehyde/sinapaldehyde) and 1410 cm^{-1} (phenolic OH bending/CH_3 bending).[25]

Tensile measurement

Tensile measurements were conducted for ring-shaped samples using a tailor-made tensile tester (ISUT-2201, Aiesu Giken, Co., Kyoto, Japan) at approximately 25 °C. Outside and inside diameters of the samples were 13.7 and 11.7 mm, respectively. The samples were stretched up to the rupture point. The stretching speed was 100 mm min^{-1}, *i.e.*, the strain speed was about 4.98 per min. A stretching ratio (α) is defined as $\alpha = l/l_0$ where α is the stretching ratio, l is a length after deformation, and l_0 is an initial length, respectively.

Laser scanning confocal microscopy

Laser scanning confocal microscopy (LSCM) was performed using a Nikon Laser Confocal Microscope System A1R with a 20× objective (numerical aperture = 0.75, CFI Plan Apochromat 20×/0.75 DIC M, Nikon Co., Japan) at r.t. The laser wavelength was 488 nm, and the detector was a single photo multiplier tube. The size of the specimen was 10 × 1 × thickness in mm^3. Three-dimensional images were also obtained with a 100× objective (CFI Plan Apochromat 100×/1.4 DIC VC, Nikon Co., Japan) using NIS-Elements software, Nikon Co., Japan. Fig. 2 shows a LSCM photograph of the sodium lignosulfonate with the fluorescence emission spectrum. The diameter of lignin powder was detected to be approximately 20–45 μm. It was also confirmed that the sodium lignosulfonate used in this study provided the wide range of detectable fluorescence spectrum from 430–750 nm, and gave the high fluorescence emission intensity at wavelength = 530 nm.

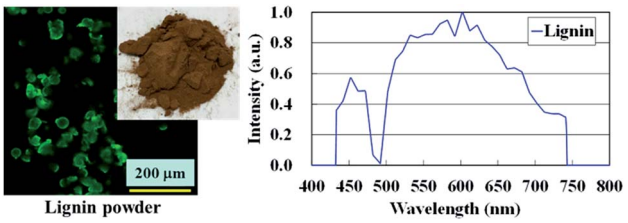

Fig. 2 LSCM photograph of the sodium lignosulfonate with the fluorescence emission spectrum.

Scanning probe microscopy

Scanning probe microscopy (SPM) observation was performed using a Bruker AXS Nanoscope III a plus D3100 (Bruker Co.) at r.t. The probes were OMCL-AC160TS (Olympus Co.). The surface of sample was prepared by cutting using an ultra-microtome (LEICA, UC6) at −100 °C.

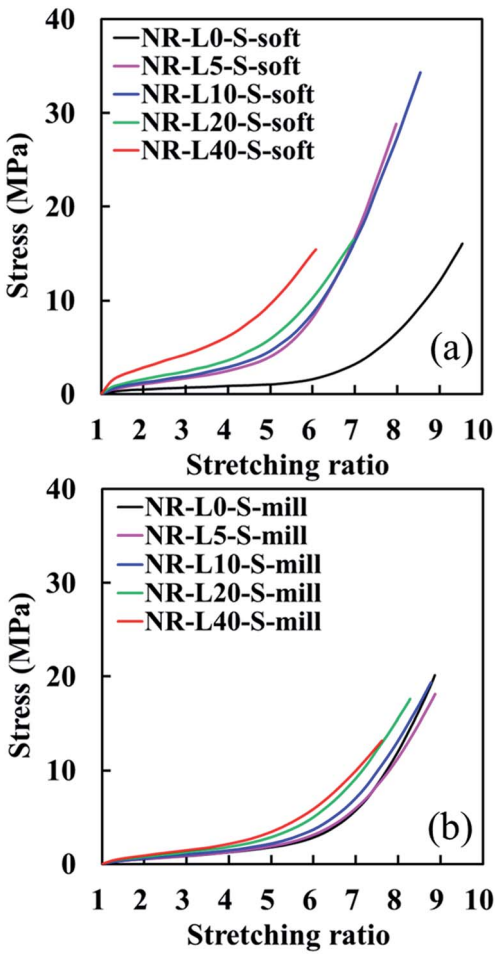

Fig. 3 Tensile stress–strain curves of the lignin-filled NR biocomposites with those of unfilled samples. (a) The soft processing and (b) the conventional mixing methods.

Evaluation of Payne effect

Payne effect was investigated at approximately 25 °C by using a rheometer MR-500 (Rheology Co., Japan) at 1 Hz of frequency and rotation angles between 0.01 and 15°. The size of the specimen was 8 × 8 × thickness in mm^3.

Dynamic mechanical analysis

Dynamic mechanical properties were evaluated using a Rheospectolar DVE-4 instrument in a tension mode at a frequency of 10 Hz and temperature range from −130 °C to 150 °C at a heating rate of 2 °C min^{-1}. The size of the specimen was 25 × 5 × thickness in mm^3. The applied static force was automatically controlled, and the dynamic strain was ±3 μm. Storage modulus (E') and loss factor (tan δ) were measured as a function of temperature.

Simultaneous wide-angle X-ray diffraction and tensile measurements

Simultaneous wide-angle X-ray diffraction (WAXD) and tensile measurements were carried out *in situ*[26,27] at BL-40XU beam line of SPring-8 in Harima, Japan.[28] A tailor-made tensile machine (ISUT-2201, Aiesu Giken, Co., Kyoto, Japan) was situated on the beam line, and WAXD patterns were recorded during tensile measurement at r.t. (approximately 25 °C). The detail of tensile measurement was same with the previous section. The samples were stretched up to the rupture point under the stretching speed of 100 mm min^{-1}. The wavelength of X-ray was 0.08322 nm and the camera length was 184.7 mm. Two-dimensional (2D) WAXD patterns were recorded using a charge-coupled device (CCD) camera (ORCA II, Hamamatsu Photonics, Co.). Intensity of the incident X-ray was attenuated using a rotating slit equipped on the beam line, and the incident beam was exposed on the sample for 70 ms every 3 s.

WAXD analysis

The obtained 2D-WAXD images were processed using "POLAR" (Stonybrook Technology & Applied Research, Inc.).[29,30] The 2D-WAXD patterns of stretched samples were decomposed into three components, *i.e.*, isotropic, oriented amorphous and crystalline components. The three components were azimuthally integrated within the range of ±75° from the equator, and crystallinity index (CI) is calculated by using eqn (2). The detail of this analytical method was described in our previous paper.[29,30]

$$\mathrm{CI} = \frac{\sum_{\text{crystal}} 2\pi \int \sin\phi \mathrm{d}\phi \int I(s)s^2 \mathrm{d}s}{\sum_{\text{total}} 2\pi \int \sin\phi \mathrm{d}\phi \int I(s)s^2 \mathrm{d}s} \quad (2)$$

here, $I(s)$ represents the intensity distribution of each peak that is read out from the WAXD pattern, s is the radial coordinate in reciprocal space in nm^{-1} unit ($s = 2(\sin\theta/\lambda)$, where λ is the wavelength and 2θ is the scattering angle), and ϕ is the angle between the scattering vector of the peak and the fibre direction.

Results and discussion

Tensile properties of lignin-filled NR biocomposites

Tensile stress–strain curves of NR biocomposites containing 5, 10, 20, and 40 phr of lignin, which were prepared by the soft processing and conventional mixing methods, are illustrated in Fig. 3 against those of unfilled samples. By repeating a few times measurements, the good reproducibility of tensile properties for all samples was obtained with the sample standard deviation (σ) < 0.382 for the stresses at the stretching ratios of 3.0, 5.0 and 7.0. Only the tensile strength (T_B) and stretching ratio at break (E_B) possessed σ < 4.16. In addition, the fracture properties have been well-known to have effects of cuts and/or scratches on the surfaces of specimens. Thus, the tensile properties using the samples with the highest T_B and E_B in Fig. 3 are summarized with their network-chain densities in Table 1. A reinforcement effect of the lignin to increase the stresses at low stretching ratios was detected in both series. Specifically, the tensile stresses of the lignin-filled NR biocomposites prepared by the soft processing method were found to significantly increase with increasing the lignin content, similar to conventional carbon black (CB)-filled systems. For example, the tensile

Table 1 Properties of lignin-filled NR biocomposites prepared by soft processing and conventional methods at different lignin contents

Sample code	Lignin content[a] (phr)	Network-chain density[b] × 10^4 (mol cm^{-3})	Stress at $\alpha = 3$ (MPa)	Stress at $\alpha = 5$ (MPa)	Stress at $\alpha = 7$ (MPa)	T_B[c] (MPa)	E_B[d]
NR-L0-S-soft	0	1.4	0.7	1.0	3.2	13.9	9.5
NR-L0-S-mill	0	1.2	0.9	1.8	5.7	18.8	8.9
NR-L5-S-soft	5	2.4	1.8	4.3	17.7	27.2	7.8
NR-L5-S-mill	5	1.2	0.9	1.9	6.0	17.1	8.8
NR-L10-S-soft	10	2.6	1.9	4.7	17.0	24.6	7.8
NR-L10-S-mill	10	1.5	1.0	2.1	7.1	19.2	8.8
NR-L20-S-soft	20	3.2	2.4	6.0	—	15.1	6.8
NR-L20-S-mill	20	1.7	1.2	2.7	8.4	17.4	8.3
NR-L40-S-soft	40	7.9	4.2	9.6	—	12.2	5.5
NR-L40-S-mill	40	2.5	1.4	3.2	9.4	11.8	7.5

[a] Parts per one hundred rubber by weight. [b] Estimated on the basis of the classical theory of rubber elasticity using eqn (1). [c] Tensile strength at break. [d] Stretching ratio at break.

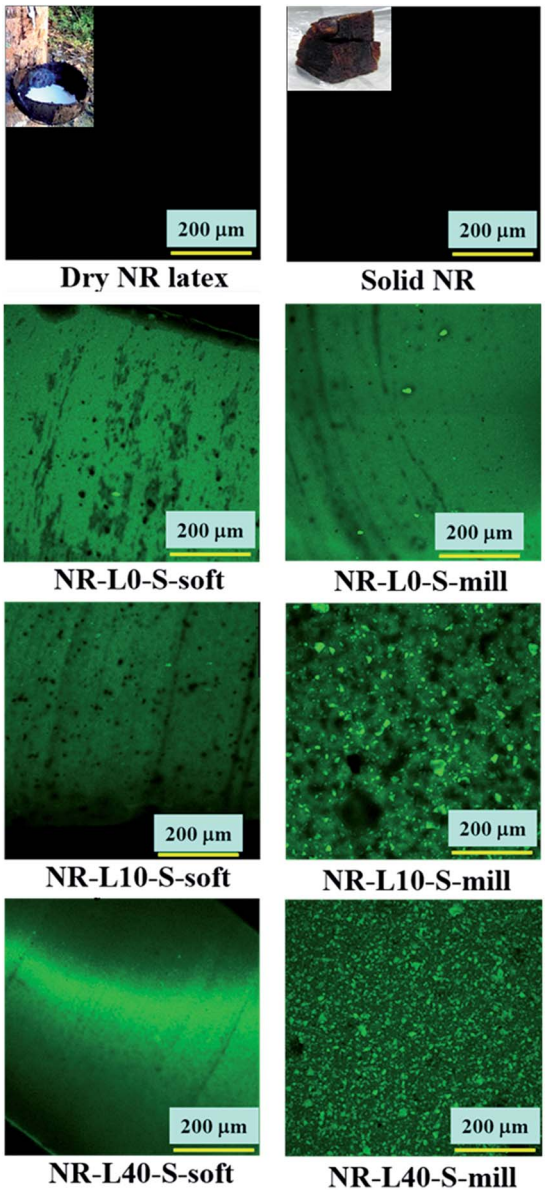

Fig. 4 LSCM images of the lignin-filled NR biocomposites, the unfilled samples, solid NR and dry NR precipitated from the latex using 10% aqueous acetic acid solution.

stresses of NR-L5-S-soft at $\alpha = 3.0$, 5.0 and 7.0 were about 160%, 330% and 450% higher than those of an unfilled sample (NR-L0-S-soft), respectively. Note that the improvement of the tensile strength and stretching ratio at break was difficult for the Lignin/NR soft biocomposites, although the soft processing was useful for the utilization of sodium lignosulfonate as a reinforcing filler for rubber. This point is our challenge in near future. On the other hand, the increment in the tensile stresses of NR-L5-S-mill was 0%, 6% and 7% at $\alpha = 3.0$, 5.0 and 7.0, respectively, when compared to unfilled NR (NR-L0-S-mill). Unlike nano-sized fillers, the direct incorporation of micron-sized lignin to the rubber matrices by conventional milling was not efficient to bring about the high performance properties even when sodium lignosulfonate with ionic sites was used.

In the lignin-filled NR biocomposites prepared by this soft processing (hereafter, it is called as "Lignin/NR soft biocomposites" in this paper), the different features of tensile properties seem to be distinguishable into two groups on the basis of the stress–strain curves. At first, NR-L5-S-soft and NR-L10-S-soft, which provided the considerably high up-turn stresses at their large strains and their stress–strain curves, were very similar. In addition, the tensile strengths of these biocomposites were surprisingly larger than that of NR-L0-S-soft. In the second, NR-L20-S-soft and NR-L40-S-soft did not show much abrupt up-turn stresses at a high strain like NR-L5-S-soft and NR-L10-S-soft, although their stresses significantly increased from the low strains. These results suggest that the reinforcement mechanism resulting from filling lignin was different for the two groups, although the processing was same among the biocomposites.

In general, the abrupt upturn of stress at high strains for cross-linked NR is ascribable to the strain-induced crystallization (SIC) behaviour. It is also well known that significant increases of tensile stresses at low strains are due to the filler–filler interaction in the composites. Therefore, the characteristics of the first group are predicted to relate to the acceleration of SIC by filling the lignin using the soft processing method. The second may be mainly concerned with a dispersion of the lignin in the rubber matrix. In order to confirm these phenomena, several characterisations were carried out for the biocomposites in this study. As already reported in a previous rapid communication on NR-L10-S-soft,[19] the soft processing was found to form the specific morphology of lignin like a filler network around the rubber phases. Thus, the morphological features of the biocomposites were compared and discussed in order to reveal the difference of the reinforcement effects between the two groups. From next section, the Lignin/NR soft biocomposites with 10 and 40 phr lignins are focused as typical samples for each group.

Morphological characteristics of Lignin/NR soft biocomposites

Morphologies of lignin in the rubber matrices of the biocomposites were investigated by using laser scanning confocal microscopy (LSCM). Fig. 4 presents the gum solid NR and the dry NR from the latex, which did not show any autofluorescence under the objective lens used in this LSCM experiment. Notably, any special treatment was not required for the samples due to an autofluorescence of lignin for the observations as explained in Fig. 2. However, the unfilled samples, *i.e.* NR-L0-S-soft and NR-L0-S-mill without the lignins also shows the fluorescence under the objective lens in this study as shown in Fig. 4. Therefore, the fluorescence phenomena were mainly ascribed to the sulfur cross-linking reagents.

On the other hand, the observed LSCM image of NR-L10-S-soft was similar to that of NR-L0-S-soft as shown in Fig. 4, even though the former contained lignin. Furthermore, the LSCM image of NR-L40-S-soft was different from those of NR-L10-S-soft and NR-L0-S-soft, where the black parts were not clearly detected, but a homogeneous green phase was instead

visible. The difference suggests two possible phenomena: the lignin may be finely dispersed in the NR matrix, and the sulfur cross-linking reagents may be well dispersed in the matrix. The considerations were apparently supported by comparing LSCM images of NR-L10-S-mill and NR-L40-S-mill. As detected in Fig. 4, NR-L10-S-mill and NR-L40-S-mill showed the fluorescence emission from both the sulfur cross-linking reagents and the lignin particles as a green background and brighter green dots, respectively. The diameter of lignin powder was found to become small by milling, and it was approximately 5–9 μm in NR-L40-S-mill. Furthermore, bigger black parts were detected in NR-L10-S-mill than in NR-L10-S-soft and NR-L0-S-soft. Since NR-L10-S-soft and NR-L40-S-soft did not show any lignin powder particles of a similar size to those detected in the lignin milled samples, these results clearly suggest the presence of better dispersion of lignin in NR-L10-S-soft and NR-L40-S-soft than in NR-L10-S-mill and NR-L40-S-mill. In addition, the size of lignin in Lignin/NR soft biocomposites was indicated to be less than 100 nm, judging from the resolution of LSCM in this study.

The three-dimensional LSCM images of NR-L40-S-soft and NR-L40-S-mill more clearly supported this consideration as shown in Fig. 5, where the lengths were approximately 120 μm, and the thickness was approximately 40 μm. The movies of these figures are shown in the journal site of ESI, video 1 and 2.† The fluorescence emissions from NR-L40-S-soft and NR-L10-S-soft may be mainly attributed to the sulfur cross-linking reagents, because the dry NR from the latex did not show any fluorescence under the objective lens used in this experimental condition. The question then is what the difference between the morphology of NR-L10-S-soft and NR-L40-S-soft is. In order to reveal the characteristic features, a scanning probe microscopy (SPM) was conducted for NR-L10-S-soft and NR-L40-S-soft in the next.

Phase and height SPM images of NR-L10-S-soft and NR-L40-S-soft are shown in Fig. 6 with those of NR-L0-S-soft. In their phase images, bright and dark parts correspond to hard and soft phases, indicating the lignin and the NR phases in NR-L10-S-soft and NR-L40-S-soft, respectively. As expected similarly to the *in situ* silica-filled NR nanocomposites prepared by the soft processing,[21,22,31,32] the lignin seemed to be located around the NR particles in the latex during formation of film, to result in the selective formation of lignin phases around the rubber phases.[19] Namely, network-like structures of lignin were detected in the biphasic structured morphologies in both NR-L10-S-soft and NR-L40-S-soft. The height images also clearly showed filler network-like structures. Note that the lignin phases became enlarged through the increase of lignin. The shape of NR particles in the latex was well reflected to the soft NR phases. Specifically, arc-shaped interfaces were clearly recognised between the lignin and rubber in NR-L40-S-soft as shown in Fig. 6. It is worth noting that the size of rubber phases of NR-L10-S-soft and NR-L40-S-soft were very similar to that of the beige coloured region of NR-L0-S-soft shown in Fig. 6, which also supported the aggregation of lignin components around the rubber particles in the NR latex. The mechanism of the formation of lignin aggregates like a network may be similar to that of the *in situ* silica network using NR latexes that has been reported previously,[22,31,32] because the lignin used in this study possesses ionic sites of sodium sulfonate. In the NR latex, the ionic sites in the lignin may have interacted with the non-rubber components of the surface of NR particles *via* Coulomb

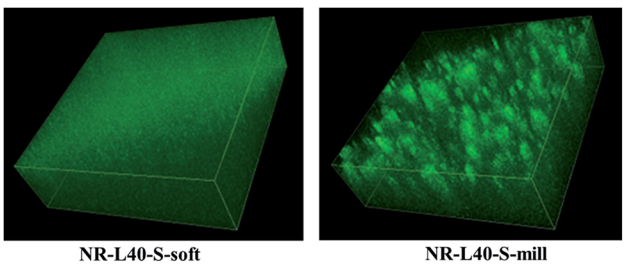

Fig. 5 Three-dimensional LSCM images of NR-L40-S-soft and NR-L40-S-mill, where the lengths and the thickness were approximately 120 μm and approximately 40 μm, respectively.

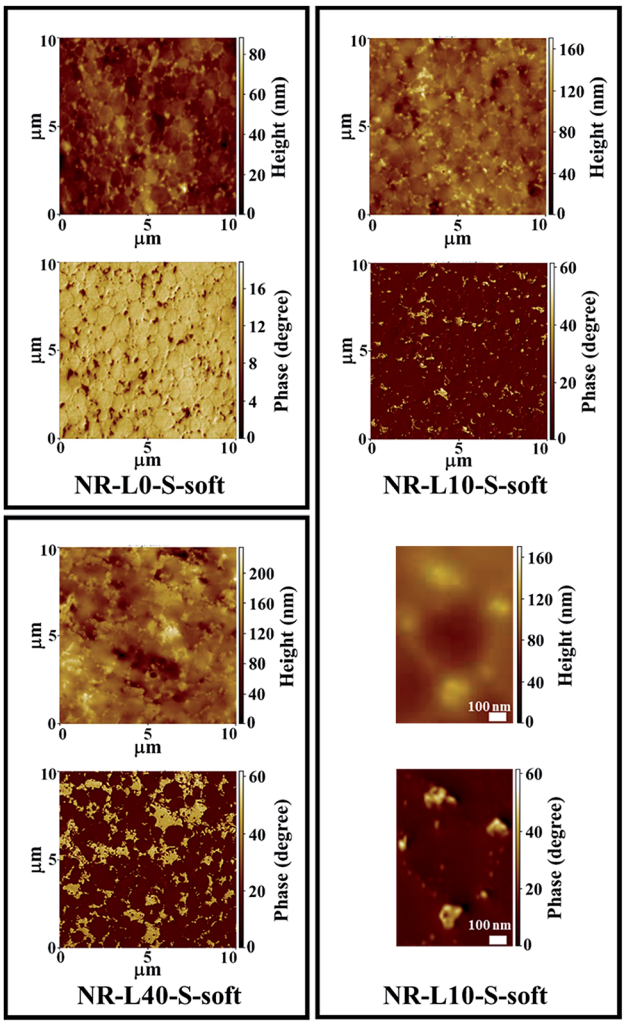

Fig. 6 SPM height and phase images of NR-L0-S-soft, NR-L10-S-soft, NR-L40-S-soft and the magnified height and phase images of NR-L10-S-soft.

interaction. In fact, the lignin around the NR phases was observed to be well wetted by NR, resulting in the unclear lignin/rubber interface shown in Fig. 6.

The SPM results of NR-L40-S-soft (rather than those of NR-L10-S-soft) clearly suggest that the organic biofiller lignin supports the following idea for the reinforcement of rubber when soft processing is utilized to prepare the nanocomposite "Not the highest dispersion but to get a certain dispersion that may be favorable to form a network-like structure of nanofiller is to be the best dispersion in terms of rubber reinforcement".[19,20] This unique morphology endowed the lignin-filled NR biocomposites prepared by the soft processing with excellent tensile properties, as shown in Fig. 3a. The network-like structure of lignin in the NR composites was confirmed by results of the Payne effect as discussed in the next section.

When the morphologies of Lignin/NR soft biocomposites and NR-L0-S-soft are compared, this unique point presented itself. The hardness of the interface phase between the rubber phases (the beige phases) changed after the filling of lignin. In the unfilled sample, the interface was softer than the rubber phases. However, the lignin made it harder than the rubber phases. This phenomenon clearly shows that the lignin plays a role in reinforcing the interface. Because sodium lignosulfonate is an organic material containing the ionic sites, the compatibility of lignin with the non-rubber components on the NR particles in the NR latex becomes good, resulting in hard layer at the interfaces after drying. In Fig. 6, it is also noted that the NR phases were spherical and/or ellipse-shaped, the size distribution was relatively homogeneous, and its average diameter was approximately 1 μm. Even after the filling of lignin, the size of NR phases was not much changed.

Generally, the rubber particles in NR latex coalesce to form a relatively strong film during drying, where the surface boundaries of the coalesced rubber particles are formed. The main components of the boundaries were reported to be non-rubber components such as phospholipids, fatty acids and so on.[33–35] Therefore, the soft phases, *i.e.* the dark brown coloured parts, which were dispersed around the NR phases of NR-L0-S-soft in Fig. 6, are supposed to be non-rubber components existing even after the sulfur cross-linking under the reaction condition of this study. Therefore, our SPM results clearly suggest that the interface ascribed to the non-rubber components was much softer than the matrix of sulfur cross-linked NR. The surfactants used for dispersing cross-linking reagents in the vulcanization may have influenced the softness of the interface.

Payne effect of Lignin/NR soft biocomposites

Generally, a difference of shear storage modulus (G') at small and large deformations reflects filler–filler interaction in the filler-filled rubber materials, known as the "Payne effect". In order to evaluate the degree of filler–filler interaction of Lignin/NR soft biocomposites, variations of G' over 10^{-2} to 10^{3}% strain at 1 Hz of frequency for the composites with 10 and 40 phr lignin content were investigated. The results are shown in Fig. 7. It is worth noting that significantly different tendencies were

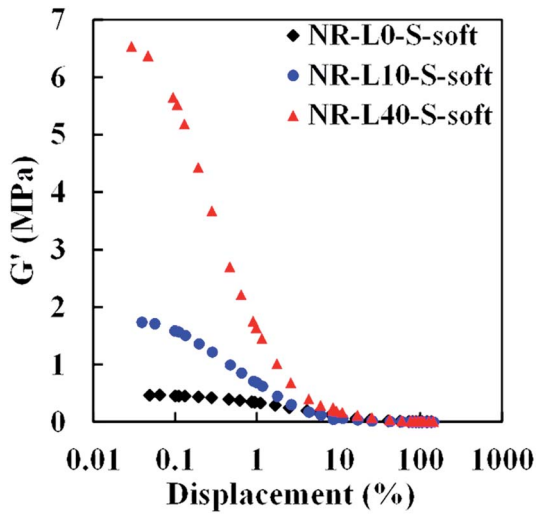

Fig. 7 Payne effect of Lignin/NR soft biocomposites.

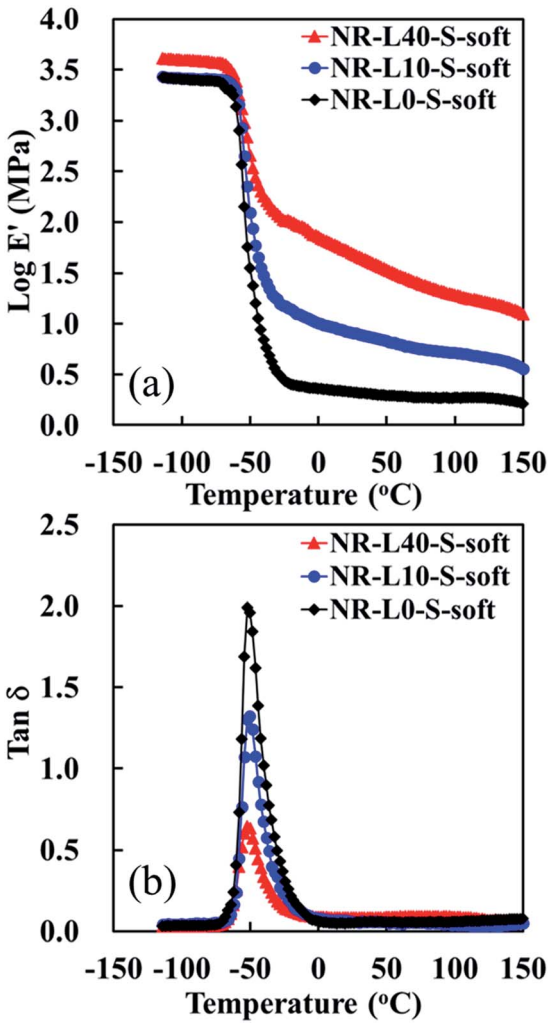

Fig. 8 Temperature dependence of (a) E' and (b) tan δ for Lignin/NR soft biocomposites.

observed among the samples. The Payne effect of NR-L40-S-soft was much larger than that of NR-L10-S-soft and NR-L0-S-soft, which agreed well with that observed for conventional carbon black or silica-filled rubber composites. The significant Payne effect of NR-L40-S-soft suggests the presence of a stiff network-like structure of lignin with high filler–filler interaction in the NR matrix. Even with the addition of a small amount of lignin by the soft processing method, the Payne effect was clearly observed, as shown in NR-L10-S-soft. The interface between the NR phases composed of the non-rubber components is supposed to be strengthened by filling of the lignin. With further increasing strain, no obvious change of the G' for Lignin/NR soft biocomposites was found, leading to the platform being subjected to a strain of 10 to 10^2%. This indicated that the filler–filler interaction of the NR biocomposites would be destroyed almost completely even in the case of NR-L40-S-soft.

Dynamic mechanical properties of Lignin/NR soft biocomposites

Fig. 8 presents the temperature dependence of the storage modulus (E') and the loss factor curve (tan δ) of Lignin/NR soft biocomposites with the unfilled sample prepared using the soft processing method. The E' at 25 °C of Lignin/NR soft biocomposites was obviously enhanced by mixing lignin, especially by the filling of 40 phr lignin. The tendency of increase of E' at 100 °C was similar to that of E' at 25 °C. These results also suggest that the NR was effectively reinforced by lignin when the soft processing method was used for preparing the rubber composites. Moreover, a reduction of the loss factor (shown as a decrease of the height of tan δ) was detected with increasing the lignin content in the NR biocomposites prepared by the soft processing method, indicating the higher restriction of movements for the rubber chains at the interface of the biphasic structures due to the higher lignin content. Therefore, it is suggested that Lignin/NR soft biocomposites provided not only the high modulus, but also high rigidity and stiffness, probably ascribed to the high filler–rubber interaction at the interface in Lignin/NR biocomposites. It is also worth noting, on the other hand, that Lignin/NR soft biocomposites show a similar identical temperature of tan δ peak at −51 °C, referring to their glass transition temperatures (T_g), with that of NR-L0-S-soft as revealed in Fig. 8. Because the lignin was located around the NR phases and the size of NR phases was similar among the samples, the T_g may be governed by the highly pure rubber phase in the core of rubber phases, not depending on the lignin contents in the samples prepared by the soft processing method.

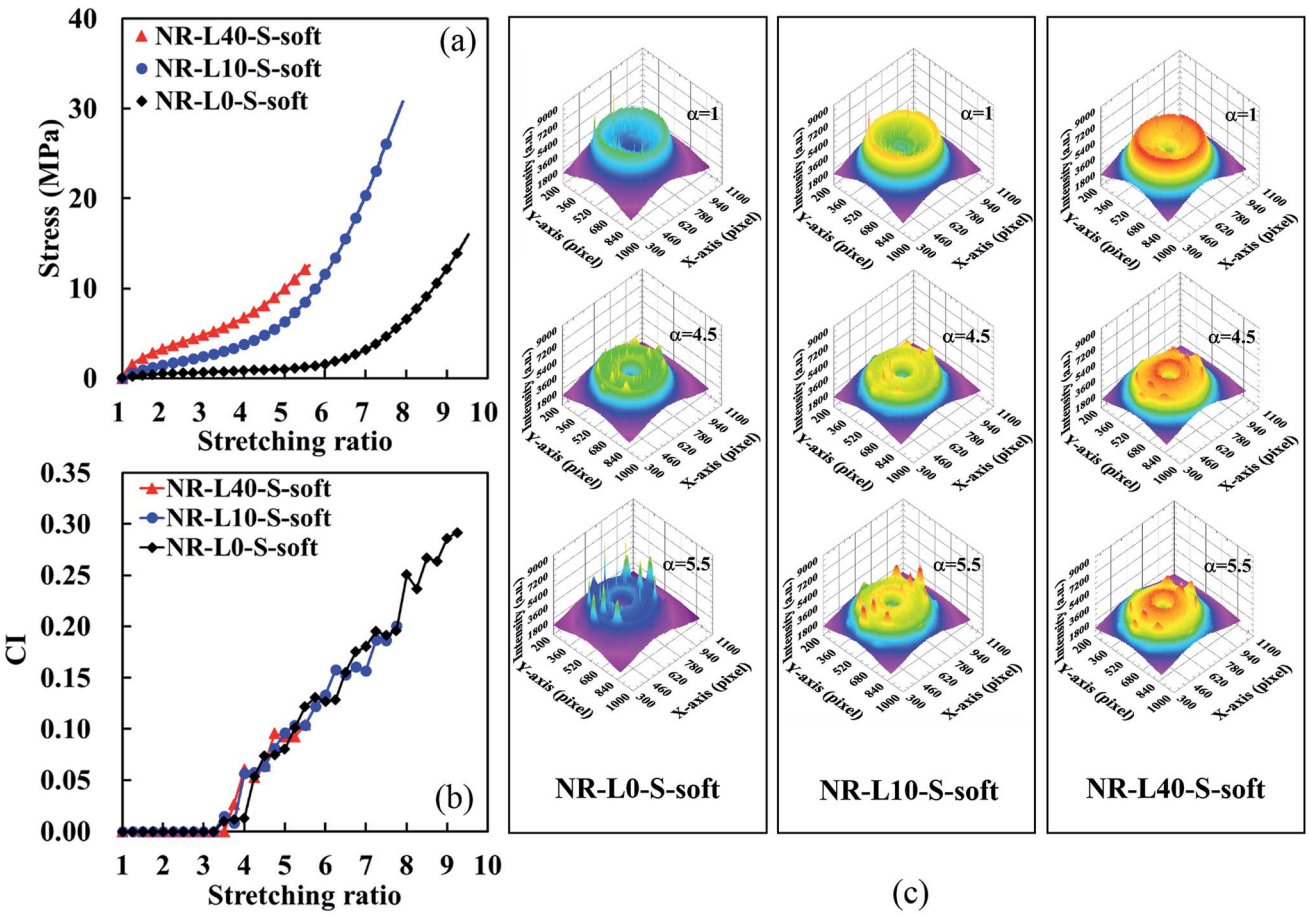

Fig. 9 SIC behaviours of Lignin/NR soft biocomposites. (a) Tensile stress–strain curves, (b) variations of crystallinity index (CI) against stretching ratio, and (c) three-dimensional WAXD patterns at $\alpha = 1$, 4.5 and 5.5.

Characteristic feature of crystallinity in the strain-induced crystallization of Lignin/NR soft biocomposites

It is well known that one of the excellent properties of NR is its significant strain-induced crystallization (SIC) behaviour. Therefore, the SIC behaviours of Lignin/NR soft biocomposites with the unique morphological features must be investigated in order to reveal the role of organic filler for the reinforcement of NR. Fig. 9 shows the tensile stress–strain curves of Lignin/NR soft biocomposites (NR-L40-S-soft and NR-L10-S-soft) and unfilled sample (NR-L0-S-soft) obtained during the simultaneous *in situ* WAXD/tensile measurements. The sequential changes of three-dimensional WAXD patterns at $\alpha = 1$, 4.5, and 5.5 are also displayed in this figure. The tensile stress–strain curves in Fig. 9a show a good reproducibility with those in Fig. 3a, where the substantial improvement of stresses by lignin was clearly observed as mentioned. Before stretching, *i.e.* $\alpha = 1$, an amorphous halo ring was observed in each WAXD pattern as shown in Fig. 9c, indicating the presence of randomly coiled amorphous chains in all samples. Upon stretching, the crystalline reflections were detected due to the SIC of NR chains along the stretching direction, and the intensities of crystalline reflections were observed to gradually increase upon further stretching. At each stretching ratio, the intensities of crystalline reflections of the WAXD patterns of NR-L40-S-soft were slightly lower than those of NR-L10-S-soft, and the crystalline reflection became broader in the former than in the latter. In order to investigate the SIC behaviours more clearly for the samples, a quantitative analysis of the crystalline reflections was conducted according to the method reported.[29,30]

Fig. 9b illustrates variations of crystallinity index (CI) against α for the Lignin/NR soft biocomposites and unfilled sample. It is worth noting that the variation of CI was approximately the same among the samples. In addition, it was clearly observed that the CI variations of all samples were stepwise upon stretching, where small plateau regions of the CI values were repeatedly detected. The stepwise SIC behaviours are supposed to be due to the unique biphasic structures in the composites prepared by the soft processing method, similarly to our previous results on *in situ* silica-filled NR composite.[21] In the case of the organic filler "lignin" in this study, the rubber particles in the NR latex also played a role as templates to locally disperse the lignin around the rubber phases. Because the size and distribution of NR particles in the latex were almost equal in all samples, it was reasonable to detect similar steps in these three samples. The reason for missing the first step in NR-L40-S-soft is probably due to the prevention of SIC by the large amounts of lignin filler around the small sized NR phases. It was also noted that the step tended to become more flat with the increase of lignin content. Unexpectedly, the degree of crystallinity upon stretching was found to be similar among the samples, and not dependent on the lignin content as described above. However, a significant difference in tensile properties was observed in Fig. 9a. This clearly means that the reinforcement effect of lignin itself appeared significantly in NR-L40-S-soft, not relating to the reinforcement effect of strain-induced crystallites. The detail of SIC behaviours of these samples will be reported elsewhere.

Conclusion

NR biocomposites with sodium lignosulfonates of 5, 10, 20, and 40 phr were successfully prepared by using the soft processing method. This method caused the rubber particles in the NR latex to act as templates for the formation of locally dispersed lignin around the rubber phases even at high levels of lignin filling. The significant Payne effect of 40 phr lignin-filled NR biocomposite suggests the presence of a stiff network-like structure of lignin with a high filler–filler interaction in the NR matrix. The Payne effect was clearly observed even by the addition of 10 phr lignin, where the interface between the NR phases composing the non-rubber components is supposed to be strengthened by lignin filling. Based on the difference of their unique morphologies, the 40 phr lignin-filled biocomposite provided better mechanical properties such as substantially higher tensile stresses, larger storage moduli, and lower dissipative loss, than the 10 phr lignin-filled biocomposite. However, low glass transition temperatures, due to the pure rubber phases, were observed in both biocomposites. This is also the characteristic of the lignin-filled NR biocomposites prepared by soft processing. The stepwise SIC was observed in both biocomposites through quick time-resolved WAXD/tensile measurements. The stepwise SIC was ascribed to the size distribution of rubber particles in NR latex in the preparation step of the biocomposites.[21] Unexpectedly, the degree of crystallisation upon stretching was similar for biocomposites with 10 phr and 40 phr lignins, up to the stretching ratio of approximately 5.5. These characteristics will be useful for developing the already promising reuse of lignin as reinforcing filler for high performance green natural rubber nanocomposites for a sustainable society.

Acknowledgements

This work was partially supported by Japan Science and Technology Agency (JST) ALCA program and a Kyoto Institute of Technology. The WAXD experiment was performed at the BL-40XU in the SPring-8 with the approval of the Japan Synchrotron Radiation Research Institute (JASRI) (Proposal No. 2014B1441). The Raman spectroscopy was kindly conducted in Thermo Fisher Scientific Inc. The authors thanks Prof. Dr S. Kohjiya, Dr A. Tohsan and Dr N. Kuhakongkiat for their useful comments.

Notes and references

1 S. Kohjiya, *Natural rubber: From the odyssey of the Hevea tree to the age of transportation*, Smithers RAPRA, Shrewsbury, 2015.
2 A. D. Roberts, *Natural Rubber Science and Technology*, Oxford University Press, Oxford, 1988.

3 L. Mullins, *The Chemistry and Physics of Rubber-Like Substances*, ed. L. Bateman, MacLaren & Sons, London, 1963, ch. 11, pp. 301–328.
4 E. H. Andrews and A. N. Gent, *The Chemistry and Physics of Rubber-Like Substances*, ed. L. Bateman, MacLaren & Sons, London, 1963, ch. 9, pp. 225–248.
5 V. K. Thakur, M. K. Thakur, P. Raghavan and M. R. Kessler, *ACS Sustainable Chem. Eng.*, 2014, **2**, 1072.
6 E. Ten and W. Vermerris, *J. Appl. Polym. Sci.*, 2015, **132**, 42069.
7 Suhas, P. J. M. Carrott and M. M. L. R. Carrott, *Bioresour. Technol.*, 2007, **98**, 2301.
8 W. Doherty, P. Mousavioun and C. Fellows, *Ind. Crops Prod.*, 2011, **33**, 259.
9 P. Wunning, *Biopolymers*, Wiley-VCH, Weinheim, 2004.
10 R. J. A. Gosselink, A. Abächerli, H. Semke, R. Malherbe, P. Käuper, A. Nadif and J. E. G. van Dam, *Ind. Crops Prod.*, 2004, **19**, 271.
11 M.-A. De Paoli and L. T. Furlan, *Polym. Degrad. Stab.*, 1985, **11**, 327.
12 C. G. Boeriu, D. Bravo, R. J. A. Gosselink and J. E. G. van Dam, *Ind. Crops Prod.*, 2004, **20**, 205.
13 C. Pouteau, P. Dole, B. Cathala, L. Averous and N. Boquillon, *Polym. Degrad. Stab.*, 2003, **81**, 9.
14 L. R. C. Barclay, F. Xi and J. Q. J. Norris, *J. Wood Chem. Technol.*, 1997, **17**, 73.
15 J. H. Lora and W. G. Glasser, *J. Polym. Environ.*, 2002, **10**, 39.
16 W. G. Glasser and S. Sarkanen, *Lignin: Properties and materials*, American Chemical Society, Washington, DC, 1989.
17 T. M. Garver and S. Sarkanen, *Renewable-resource materials: New polymer sources*, ed. C. E. Carraher Jr and L. H. Sperling, Plenum Press, New York, 1986, pp. 287–304.
18 C. Jiang, H. He, X. Yao, P. Yu, L. Zhou and D. Jia, *J. Appl. Polym. Sci.*, 2015, **132**, 42044.
19 T. Phakkeeree, Y. Ikeda, H. Yokohama, P. Phinyocheep, R. Kitano and A. Kato, *J. Soc. Fiber Sci. Technol.*, 2016, **72**, 160.
20 A. Kato, A. Tohsan, S. Kohjiya, T. Phakkeeree, P. Phinyocheep and Y. Ikeda, *Progress in Rubber Nanocomposites*, Woodhead/Elsevier, ch. 12, 2016.
21 Y. Ikeda and A. Tohsan, *Colloid Polym. Sci.*, 2014, **292**, 567.
22 A. Tohsan, R. Kishi and Y. Ikeda, *Colloid Polym. Sci.*, 2015, **293**, 2083.
23 H. Chung and N. R. Washburn, *Green Mater.*, 2012, **1**, 137.
24 L. R. G. Treloar, *The physics of rubber elasticity*; Clarendon Press, Oxford, 1975.
25 U. P. Agarwal, J. D. McSweeny and A. S. Ralph, *J. Wood Chem. Technol.*, 2011, **31**, 324.
26 Y. Ikeda, Y. Yasuda, S. Makino, S. Yamamoto, M. Tosaka, K. Senoo and S. Kohjiya, *Polymer*, 2007, **48**, 1171.
27 Y. Ikeda, Y. Yasuda, K. Hijikata, M. Tosaka and S. Kohjiya, *Macromolecules*, 2008, **41**, 5876.
28 SPring-8 Web site, http://www.spring8.or.jp/en/.
29 M. Tosaka, S. Murakami, S. Poompradub, S. Kohjiya, Y. Ikeda, S. Toki, I. Sics and B. S. Hsiao, *Macromolecules*, 2004, **37**, 3299.
30 M. Tosaka, S. Kohjiya, S. Murakami, S. Poompradub, Y. Ikeda, S. Toki, I. Sics and B. S. Hsiao, *Rubber Chem. Technol.*, 2004, **77**, 711.
31 A. Tohsan, P. Phinyocheep, S. Kittipoom, W. Pattanasiriwisawa and Y. Ikeda, *Polym. Adv. Technol.*, 2012, **23**, 1335.
32 A. Tohsan and Y. Ikeda, *Chemistry, manufacture and applications of natural rubber*, ed. S. Kohjiya and Y. Ikeda, Woodhead/Elsevier, Cambridge, 2014, ch. 6, pp. 168–192.
33 D. C. Blackley, *Polymer Lattices Science and Technology*, Chapman & Hall, London, 1997, vol. 2.
34 K. Nawamawat, J. T. Sakdapipanich, C. C. Ho, Y. Ma, J. Song and J. G. Vancsod, *Colloids Surf., A*, 2011, **390**, 157.
35 J. Sakdapipanich, R. Kalah, A. Nimpaiboon and C. C. Ho, *Colloids Surf., A*, 2015, **466**, 100.